Fractional non-Brownian motion and trapping-time distributions of grains in rice piles

K. I. Hopcraft, R. M. J. Tanner, E. Jakeman, and J. P. Graves
Theoretical Mechanics Division, School of Mathematical Sciences, University of Nottingham, University Park, Nottingham, NG7 2RD, United Kingdom
(Received 26 January 2001; published 24 July 2001)

Non-Gaussian height fluctuations occurring on the fueling time scale of a slowly driven rice pile match those observed in some turbulent/critical phenomena, forming an anticorrelated random fractal process with Hurst exponent $H=0.2$. Inspired by this observation, the concept of fractional Brownian motion (FBM) is extended to treat stochastic processes with skewed increments. Simulations of this process for antipersistent motion have first return time distribution deviating from the t^{-2+H} law for FBM. The first return time distribution of this fractional non-Brownian motion describes and quantitatively determines the trapping-time distribution of grains in rice piles upon incorporating a continuous representation of the additional height fluctuations that occur on the time scale between fueling events.

DOI: 10.1103/PhysRevE.64.026121 PACS number(s): 02.50.−r, 89.75.Da, 05.65.+b

I. INTRODUCTION

Sand piles [1] or rice piles [2,3] have become model paradigms for self-organized critical (SOC) phenomena in nonequilibrium complex systems, and SOC has been used to describe physical [4], biological [5], and economic [6] behaviors, among others [7]. The models are rules for redistribution of a physical quantity to nearest neighbor locations once a local nonlinear stability threshold is exceeded, under slow, continuous driving. The complex behaviors that obtain have prompted workers to seek links between SOC and stable random processes [8]. Non-Gaussian stable laws [9] have probability density functions (PDF's) possessing power-law tails $p(x)\sim x^{-\nu}$ with indices in the range $1\leqslant\nu<3$, so the variance and higher moments of the distributions do not exist. One property used to characterize rice-pile phenomenology occurs on the fueling time scale and is the time a grain remains at rest before being transported to another site—the ''trapping time.'' Experiments and simulations [2,3] have PDF's for these trapping times with tails of index $\nu\approx 2.16$ falling within that part of the stable regime for which a mean trapping time exists. Although scaling arguments have been invoked to collate different system sizes and rice-pile algorithms within universality classes, the reasons why the trapping-time distribution is apparently asymptotically stable and ν adopts specific values have not been explained nor related to the microdynamics of the system. This paper sheds light on these two issues through linking the PDF of trapping times to the distribution of first returns of a random walk whose increments represent the fluctuations in the height of the pile occurring on two separate time scales.

A quantitative determination of the value of ν requires implementing different diagnostics in a rice-pile cellular automaton to ascertain the form of fluctuations in the height of the pile and their correlation properties. These diagnostics reveal that the height of the pile, when viewed on the fueling time scale, is described by a fractal random process with non-Gaussian increments. It will be argued that the trapping-time distribution is equivalent to the first return time of this random process, and its description requires broadening the concept of fractional Brownian motion (FBM) to one with skewed increments. The first return distribution of this ''fractional non-Brownian motion'' (FNBM) differs from that for FBM. Further diagnostics examine the height fluctuations occurring on the intrafueling time scale occurring between fueling events. These fluctuations modify the FNBM by terminating longer trapping times and provide quantitative agreement with cellular automaton data.

Fractional Brownian motion [10] describes the trajectory of a particle whose increments have a Gaussian distribution. The Hurst exponent H measures the degree of correlation in the random walk constructed from these increments. Persistence or antipersistence occurs if H is greater or less than $\frac{1}{2}$, respectively, and Brownian motion occurs when $H=\frac{1}{2}$. For a particle undergoing FBM, the distribution of first return has a stable-law tail with index $\nu=2-H$ [11], being exactly stable when $H=\frac{1}{2}$ [12].

Were the height of a pile executing FBM, the time for a grain to return to the surface would have a distribution with index in the range $1<\nu\leqslant 2$. A grain can move and thereby end its trapping time only when at the surface of the pile; hence the trapping-time distribution should match that for the first return time. This observation is contradicted by the measured values, which have $\nu>2$, for both experiment and simulation. Thus the height of the pile cannot be described by a FBM. This deduction is borne out in what follows by delineating the competing effects that result from the skewness of the distribution of height fluctuations occurring on the fueling time scale and the modifications introduced by the fluctuations occurring on the intrafueling time scale.

In the following section, the rice-pile cellular automaton is briefly described and the height fluctuations of the pile and their correlation properties obtained and fitted to a model. Section III describes the technique used for obtaining the continuous stochastic process that determines these fluctuations and the results of computer simulations of this process which are used to obtain the first return time distribution. Section IV considers how the height fluctuations occurring on the intrafueling time scale alters the first return distribution. The final section summarizes the main results and briefly discusses the implications. Technical details of how

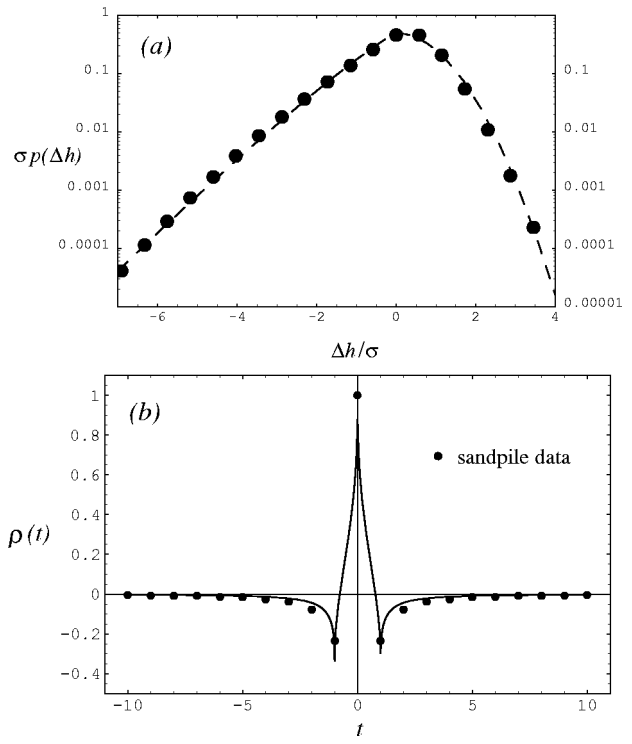

FIG. 1. The PDF of Δh for the cellular automaton on the fueling time scale are shown by data points in (a), and the dashed line is Eq. (1). Data points in (b) show $\rho(t)$ for the height changes. The solid line is Eq. (2) with $H=0.2$.

the continuous non-Gaussian stochastic process is obtained from a suitably correlated Gaussian process are assigned to the Appendix.

II. HEIGHT FLUCTUATIONS OF A RICE PILE ON THE FUELING TIME SCALE

The rice-pile cellular automaton, whose rules are described in [3], retains the identity of any grain in the pile, and so sophisticated diagnostics can be applied to elucidate the various behaviors it produces. One such diagnostic is the height change Δh between consecutive fuelings, which is monitored for all sites in the pile beyond the location of the central fueling point.

The PDF of Δh, shown by data points in Fig. 1(a), is stationary and independent of the pile size. It has zero mean, variance $\langle \Delta h^2 \rangle = \sigma^2 = 3.01$, and skewness coefficient $s = \langle \Delta h^3 \rangle / \sigma^{3/2} \approx -0.94$. These height fluctuations have a distribution similar to that describing experimentally measured fluctuations of a confined turbulent flow and numerically calculated critical behavior in a ferromagnet [13]. The PDF

$$p(\Delta h) = \begin{cases} A \exp(-|\Delta h/\alpha c|^{\beta}), & \Delta h < 0 \\ A \exp(-|\Delta h/c|^{\mu}), & \Delta h \geqslant 0 \end{cases} \qquad (1)$$

adequately models these data and is shown by the dashed line in Fig. 1(a) for $\beta = 1.13$, $\mu = 1.98$, with constants A, α, and c determined by stipulating that the PDF have unit normalization, zero mean, and variance σ^2, viz.,

$$A = [c\Gamma(1+1/\mu) + \alpha c \Gamma(1+1/\beta)]^{-1},$$

$$\alpha = \left(\frac{\Gamma(1+2/\mu)}{\Gamma(1+2/\beta)} \right)^{1/2},$$

$$c^2 = \sigma^2 \left(\frac{\Gamma(1+1/\mu) + \alpha \Gamma(1+1/\beta)}{\Gamma(1+3/\mu) + \alpha^3 \Gamma(1+3/\beta)} \right),$$

with $\Gamma(\beta)$ the Gamma function.

Another diagnostic that can be applied measures the correlation properties of the height fluctuations. Data points in Fig. 1(b) show the autocorrelation function $\rho(t) = \langle \Delta h(t) \Delta h(0) \rangle / \sigma^2$, where the time lag is measured in fueling events and the angular brackets denote an ensemble average over the same sites as those for which the PDF (1) is valid. Assuming the height h of the pile is a (nonstationary) fractal process with structure function $\langle [h(t) - h(0)]^2 \rangle \sim 2|t|^{2H}$ yields an autocorrelation function for the (stationary) increments

$$\rho(t) = \frac{1}{2}(|1+t|^{2H} + |1-t|^{2H} - 2|t|^{2H}), \qquad (2)$$

and the curve that results is shown by the solid line in Fig. 1(b) for when $H = 0.2$.

The autocorrelation function (2) satisfies

$$\int_{-\infty}^{\infty} dt' \rho(t') = \begin{cases} 0, & H < 1/2 \\ 1, & H = 1/2 \\ \infty, & H > 1/2 \end{cases}$$

and has power-law memory for large times with $\rho(t) \sim H(2H-1)t^{2(H-1)}$. These two results indicate that the process is antipersistent if $H < \frac{1}{2}$. An anticorrelated fractal process therefore accurately describes height changes of the pile on the fueling time scale. The first return distribution of such random motion will now be considered.

III. THE FIRST PASSAGE DISTRIBUTION OF NON-GAUSSIAN CORRELATED NOISE

Although algorithms exist for generating FBM with prescribed H (e.g., [14]), these are inapplicable to motions with non-Gaussian increments. Indeed, until very recently it has been impossible to rigorously generate noise having arbitrary, exponentially bounded single interval statistics and prescribed autocorrelation function. The ''memoryless nonlinear transformation'' (MNLT) [15] enables such noise to be formed from a suitably correlated Gaussian random process, for which the method of generation by Fourier synthesis is known (e.g., [16]). Details of the MNLT technique are assigned to the Appendix.

A lengthy but straightforward calculation following Ref. [15] obtains the result

$$\rho(t)=\frac{1}{2\pi}\sum_{n=0}^{\infty}\frac{r_G(t)^n}{2^n n!}\times\left(\int_{-\infty}^{\infty}dx\,\exp(-x^2/2)H_n(x/\sqrt{2})\Delta h(x)\right)^2 \quad (3a)$$

where

$$\Delta h(x)=\begin{cases}\alpha c\left\{\Gamma_{1/\beta}^{-1}\left(\dfrac{(1-\mathrm{erfc}[x/\sqrt{2}]/2)}{A\alpha c\Gamma(1+1/\beta)}\right)\right\}^{1/\beta}, & x<x_c\\ c\left\{\Gamma_{1/\mu}^{-1}\left(\dfrac{\mathrm{erfc}(x/\sqrt{2})}{2Ac\Gamma(1+1/\mu)}\right)\right\}^{1/\mu}, & x\geqslant x_c\,.\end{cases} \quad (3b)$$

The variable $x_c=\sqrt{2}\,\mathrm{erfc}^{-1}(2Ac)$, and $\Gamma_\mu^{-1}(x)$ is the inverse of the "regularized" incomplete Gamma function, defined through $\Gamma_\mu(x)=1/\Gamma(\mu)\int_x^\infty du\,u^{\mu-1}\exp(-u)$. Equation (3a) expresses the non-Gaussian correlation function $\rho(t)$ as a power series of terms involving the Gaussian correlation function $r_G(t)$ which can be used to obtain $r_G(t)=r_G(\rho(t))$. Equation (3b) provides the mapping for generating random numbers with PDF (1) from a standard Gaussian random variable x.

To illustrate the modifications to FBM caused by skewed increments, such as those described by Eq. (1), consider fixing the mean, variance, and μ to the values given above and use β as the variable to control the skewness of the process through

$$s=\frac{3^{3/2}[\Gamma(1+4/\mu)-\alpha^4\Gamma(1+4/\beta)][\Gamma(1+1/\mu)+\alpha\Gamma(1+1/\beta)]^{1/2}}{[\Gamma(1+3/\mu)+\alpha^3\Gamma(1+3/\beta)]^{3/2}}.$$

A non-Gaussian process $\{\Delta h(t)\}$ with correlation function $\rho(t)$ can be derived from a Gaussian process $\{x(t)\}$ with zero mean, unit variance, and correlation function $r_G(t)$, in the following way. First a sequence of uncorrelated Gaussian random numbers is generated using any standard method. The correlation function of the non-Gaussian process given by Eq. (2) is used in conjunction with Eq. (3a) to obtain the correlation function of the Gaussian process $r_G(t)=r_G(\rho(t))$, the inversion being performed numerically. This is then used to generate a sequence of correlated Gaussian random numbers $\{x(t)\}$ by the Fourier synthesis method [16]. These random numbers are used as inputs in Eq. (3b) to form a sequence of non-Gaussian random numbers $\{\Delta h(t)\}$ that have the correct autocorrelation function $\rho(t)$. With these correlated non-Gaussian random numbers, the fractional non-Brownian motion

$$\zeta(t_n)\equiv h(t_n)-\langle h\rangle=\sum_{j=1}^{n}\Delta h(t_j) \quad (4)$$

is formed.

The first return time distribution of ζ, or "down crossings," gives the epochs for which $\zeta>0$. In the context of the rice pile, these epochs can be interpreted as the time between the burial of a grain and its reemergence at the surface of the pile. The PDF $p(t,s)$ for the times between an up and a down crossing have a power law with index $\nu=2-H-f(s,H)$, as confirmed in Fig. 2, which displays the deviation of the tail of the return time distribution from that for FBM for a subset of all the results. Plotting $t^{2-H}p(t,s)$ as a function of t for $H=0.2$ and $s=0$, -0.94, and -1.75 and then fitting the data to a line using least squares obtains $f(s,H)$. Figure 3 shows $f(s,H)$ as a function of s for two values of H. In both cases f is symmetric about $s=0$, being necessarily zero at $s=0$ when the motion reverts to FBM. The open circles are for $H=0.2$, the star corresponds to parameters for the rice-pile simulation, and the filled circles are for $H=0.35$. For larger absolute values of s,f saturates in both instances, although the saturation value decreases as $H\rightarrow 1/2$. This is to be expected because the motion must necessarily be Brownian when $H=1/2$ by virtue of the central limit theorem [12], and this observation is confirmed by the simulations. For values $H>1/2$, $f\equiv 0$ and so the return times remain the same as those for FBM. Thus the skewness of the underlying process effectively enhances the value of H appearing in the exponent for the return times for $H<1/2$.

The data forming each point in Fig. 3 are determined from $\sim 10^6$ realizations and each point in the diagram is obtained using the technique exemplified by Fig. 2 from a power-law tail extending over 3.3 decades. This exceeds the 3 decades of power-law behavior displayed in [11]. The simulations are

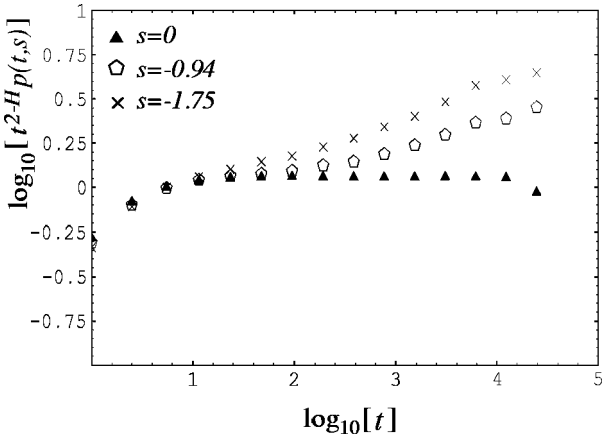

FIG. 2. Data for $s=-0.94$ and $s=-1.75$ show the deviation of the return time distribution from FBM ($s=0$) on the fueling time scale. The Hurst exponent $H=0.2$ in each case.

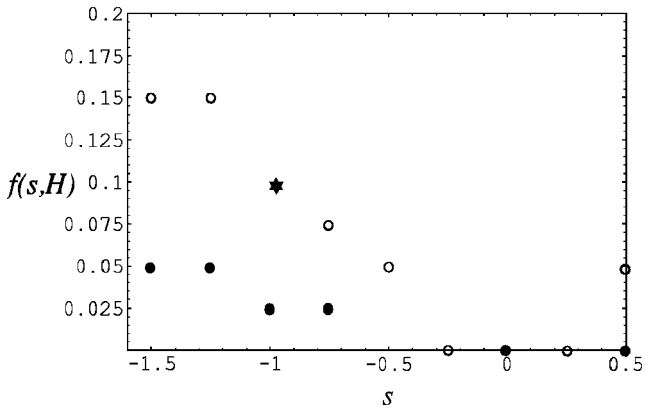

FIG. 3. The function f appearing in the exponent for the return time distribution as a function of s. Open circles are for $H=0.2$. The star denotes the value for the simulation. The filled circles are for $H=0.35$.

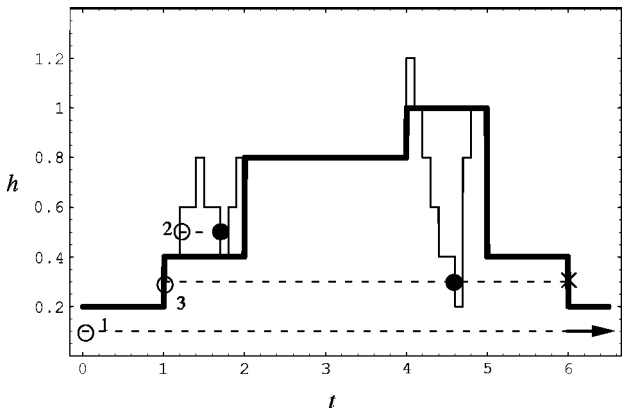

FIG. 4. Schematic of height fluctuations (arbitrary units) at a single site on the fueling (thick lines) and intrafueling (thin lines) time scales.

insensitive to finite step-size effects. Inaccuracies induced by these would manifest themselves as a biasing of the random walk, being especially evident when $H>1/2$. None of the simulations exhibit such a drift for any value of H considered and the process $\zeta(t)$ has zero mean throughout. Considering the time between an up and down crossing gives the distribution of times for which $\zeta<0$ and this has identical distribution to the times for which $\zeta>0$. Indeed, this must be so because both $\Delta h(t)$ and $\zeta(t)$ have zero mean, and so the average amount of time the processes remain in either a positive or negative state is identical. However, this situation is only true for returns to the initial location. The distribution of times for a sojourn between a level crossing $a\neq 0$ will depend upon whether $\zeta>a$ or $\zeta<a$.

Inserting appropriate parameter values for the rice-pile simulation gives $\nu=2-0.2-0.1=1.7$, and this still differs from the observed value of $\nu\sim 2.16$. However, this FNBM occurs on the fueling time scale and does not account for the additional fluctuations in height that occur between feeds. These fluctuations are described in the next section and incorporated into the random walk.

IV. MODIFICATIONS ON THE INTRAFUELING TIME SCALE

Figure 4 is a schematic of the temporal fluctuations in height at a single site. The thick and thin lines depict height fluctuations on the fueling and intrafueling time scales, respectively. The dashed horizontal lines show those periods for which particular grains are trapped. Grain 1 is buried at the start of the section and remains so throughout. Grain 2 arrives at the site between the first and second feeds, and is trapped for a short period before further activity on the intrafueling time scale brings it to the surface, whereupon it is ejected at $t\sim 1.7$. Recall that the trapping time occurs on the fueling time scale; hence, because the grain was buried and disinterred within the same time step, its trapping time is zero and does not contribute to the distribution. Contrast this with grain 3, which is buried at $t=1$ and would move off at $t=6$ if the FNBM were to apply exclusive of any other effects. However, this neglects the intrafueling time scale fluctuations that terminate the trapping time at $t\sim 4.6$. Thus the FNBM overestimates the length of trapping times through not accounting for downward excursions in the height of the pile on the intrafueling time scale. Upward excursions of the pile do not affect the dynamics.

The points in Fig. 5 show the PDF for the maximum downward excursion for the height of the pile δh on the intrafueling time scale produced by the cellular automaton, which has standard deviation $\sigma_{\delta h}=0.66$. The distribution is discrete because the height of the pile is measured in numbers of grains. The solid line is a continuous fit to this PDF having the form $P(\delta h)=B\exp[-g(\delta h)]$ where $g(\delta h)$ is a ninth order polynomial in odd powers of δh and B provides the normalization for the continuous representation. The continuous FNBM Eq. (4) is monitored and subjected to additional height decrements whose frequency is determined by $P(\delta h)$. If the additional fluctuations cause $\zeta(t)<0$ the trapping time is terminated, whereas if $\zeta(t)>0$ throughout the FNBM continues on the fueling time scale. The distribution of first return times is shown by the full line in Fig. 6. This is a power law with index $\nu\sim 2.16$ for times $2\lesssim t\lesssim 200$, which matches the result for the cellular automaton. For longer

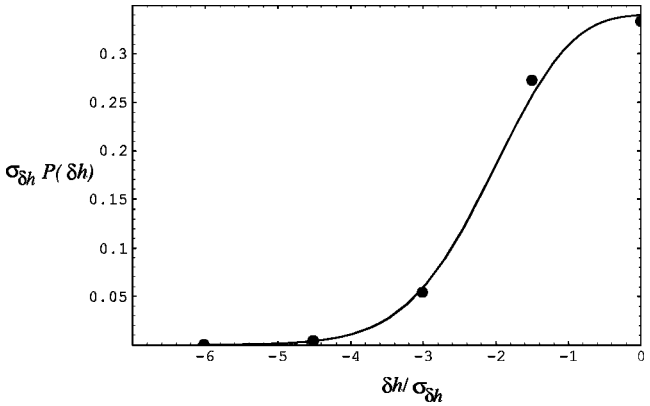

FIG. 5. PDF for downward fluctuations in height on the intrafueling time scale where dots are data from the simulation. The full curve is the function fit.

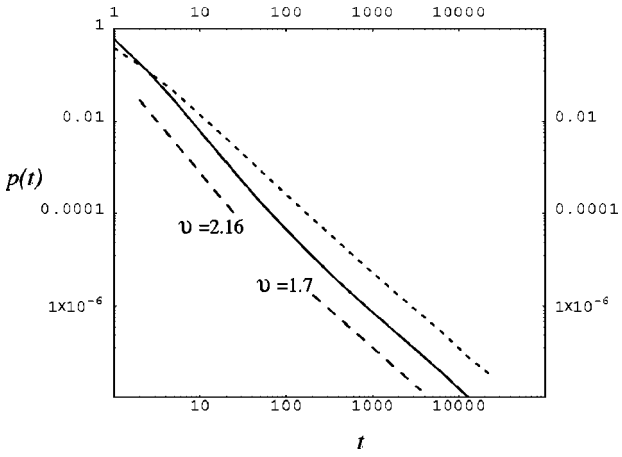

FIG. 6. Return time distribution for the FNBM modified by the intrafueling time scale fluctuations. The parameters used are those obtained from the rice-pile data: $s=-0.94$, $H=0.2$. The power-law tail has index $\nu=2.16$ for shorter return times in accord with the rice-pile data. The short dashed line shows the analogous return time distribution without additional fluctuations and has tail index 1.7.

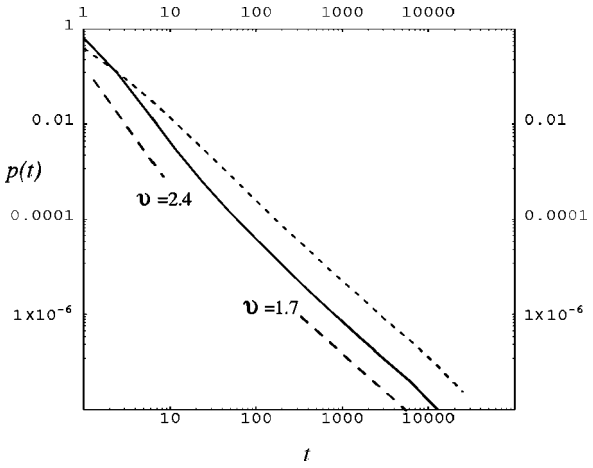

FIG. 7. Return time distribution for the FNBM modified by uniformly distributed intrafueling time scale fluctuations with all the parameters as in Fig. 6. The power-law tail has index $\nu\sim2.4$ for shorter return times.

times the power law increases to $\nu\sim1.7$, which is the same as the index for the FNBM without the intrafueling time scale modifications, shown by the long dashed line. This is to be expected because the FNBM describes diffusive trajectories that can attain arbitrarily large distances from the origin where the intrafueling time scale fluctuations have no effect in modifying the motion. The skewness of the height fluctuations is an important ingredient, for if these were modeled by FBM with the same correlation properties and intrafueling time scale fluctuations, the distribution of the first return times would have $\nu\sim2.26$, which *overestimates* the index.

Performing the simulation again but with a different $P(\delta h)$ illustrates the importance of the form adopted by the intrafueling time scale fluctuations for the distribution of return times. For example, choosing $P(\delta h)$ to be a uniform distribution with the same mean as that described by the cellular automaton gives the return time distribution shown in Fig. 7. For times in the range $2\lesssim t\lesssim100$ the index ν is strongly modified to ~2.4. Thus random walks are more effectively terminated upon incorporating uniformally distributed intrafueling time scale fluctuations. For longer times the power law increases to $\nu\sim1.7$ as before.

V. SUMMARY AND CONCLUSIONS

This paper has sought to clarify the reason for the occurrence of heavy tailed trapping-time distributions obtained in rice-pile experiments and cellular automata simulations. The trapping time is equivalent to the time a grain remains buried beneath the surface of the pile, and the distribution of these times is therefore equivalent to the first return time distribution of the height fluctuations of the pile. When measured on the fueling time scale, the height fluctuations are described by a skewed, antipersistent, fractal random process whose return time distribution differs from that for fractional Brownian motion. The skewness of the distribution of increments effectively enhances the Hurst exponent for antipersistent motion, but has no effect when the motion is persistent. To obtain a match between the indices characterizing rice-pile data and fractional non-Brownian motion requires incorporating into FNBM additional fluctuations in height occurring on the intrafueling time scale, the effect of which is to terminate the longer trapping times and therefore raise the value of the index. The shape of the distribution of these additional fluctuations affects the value of the index characterizing the power-law tail and this observation presents the opportunity for fashioning systems to have particular properties or outcomes.

The distribution depicted in Fig. 1(a) is similar to that describing fluctuation phenomena in experimentally measured and simulated complex systems [13]. Common features of these systems are finite size, open boundaries, dissipation, and the existence of inner and outer scale sizes for the fluctuations. In the present context this distribution relates to extremal fluctuations and it is, perhaps, suggestive that the PDF Eq. (1) is similar to the error distribution [17]. However, the possible universality of this PDF is not the point of central interest here. Rather it forms but one element in a complex chain from which Lévy-like statistics ultimately obtain.

Additional materials including animations of the cellular automaton can be viewed at http://spencer.nott.ac.uk/~etzrt/index.html

ACKNOWLEDGMENTS

This work was supported by the United Kingdom Engineering and Physical Science Research Council and by the Leverhulme Trust.

APPENDIX: MNLT TECHNIQUE

The MNLT technique works by first equating the cumulative distribution of a Gaussian process with zero mean and

unit variance to the cumulative distribution of the non-Gaussian process, i.e.,

$$\int_{\Delta h}^{\infty} dy\, p(y) = \frac{1}{(2\pi)^{1/2}} \int_{x}^{\infty} dx' \exp(-x'^2/2) = \frac{1}{2}\,\mathrm{erfc}(x/\sqrt{2})$$

with $\mathrm{erfc}(x)$ the complementary error function [18]. The complementary quantile function $Q(\Delta h)$ of the non-Gaussian process, defined through

$$\int_{Q(\Delta h)}^{\infty} dy' p(y') = \Delta h,$$

is used to construct a transformation that maps the input Gaussian random values $x(t)$ to the output non-Gaussian random values $\Delta h(t)$:

$$\Delta h(t) = Q\left(\frac{1}{2}\,\mathrm{erfc}[x(t)/\sqrt{2}]\right).$$

For the distribution of the height changes given by Eq. (1) the complementary quantile function is

$$Q(\Delta h) = \begin{cases} \dfrac{Ac}{\beta}\Gamma\left(\dfrac{1}{\beta}, \left(\dfrac{\Delta h}{\alpha c}\right)^{\beta}\right), & \Delta h \geqslant 0 \\ 1 - \dfrac{A\alpha c}{\mu}\Gamma\left(\dfrac{1}{\mu}, \left(\dfrac{\Delta h}{c}\right)^{\mu}\right), & \Delta h < 0, \end{cases}$$

where $\Gamma(a,x)$ is the incomplete Gamma function [18]. Equations (3b) result upon inverting these expressions.

The correlation function of the non-Gaussian process can now be expressed in terms of a joint Gaussian process with autocorrelation function $r_G(t)$ and distribution P_G upon using:

$$\rho(t) = \frac{\langle \Delta h(t)\Delta h(0)\rangle}{\sigma^2} = \int_{-\infty}^{\infty} dx' \int_{-\infty}^{\infty} dx'' \Delta h(x')\Delta h(x'') P_G(x', x'', r_G(t)).$$

The integrals can be performed upon expressing the joint Gaussian distribution as an expansion in terms of Hermite polynomials $H_n(x)$ [18],

$$P_G(x', x'', r_G(t)) = \frac{\exp[-\frac{1}{2}(x'^2 + x''^2)]}{2\pi} \times \sum_{n=0}^{\infty} \frac{H_n(x'/\sqrt{2}) H_n(x''/\sqrt{2})}{2^n n!} r_G(t)^n,$$

whence the result (3a) in the text.

[1] P. Bak, C. Tang, and K. Wiesenfeld, Phys. Rev. Lett. **59**, 381 (1987).

[2] K. Christensen, Á. Corral, V. Frette, J. Feder, and T. Jøssang, Phys. Rev. Lett. **77**, 107 (1996); V. Frette, K. Christensen, A. Malthe-Sørenssen, J. Feder, and T. Jøssang, Nature (London) **379**, 49 (1996).

[3] M. Boguñá and Á. Corral, Phys. Rev. Lett. **78**, 4950 (1997).

[4] P. Bak, C. Tang, and K. Wiesenfeld, Phys. Rev. A **38**, 364 (1988); K. Christensen and S.R. Nagel, Rev. Mod. Phys. **64**, 321 (1992); S. Mineshige, M. Takeuchi, and H. Nishimori, Astrophys. J. **435**, L125 (1994); D.H. Zanette and P.A. Alemany, Phys. Rev. Lett. **75**, 366 (1995); R.D. Pinto, W.M. Gonçalves, J.C. Sartorelli, and M.J. de Oliveira, Phys. Rev. E **52**, 6896 (1995); R.O. Dendy and P. Helander, Plasma Phys. Controlled Fusion **39**, 1947 (1997).

[5] *On Growth and Form*, edited by H.E. Stanley and N. Ostrowsky (Nijhoff, Dordrecht, 1986); B.J. Cole, J. Anim. Beha. **50**, 1317 (1995); G.M. Viswanathan, V. Afanasyev, S.V. Buldyrev, E.J. Murphy, P.A. Prince, and H.E. Stanley, Nature (London) **381**, 413 (1996).

[6] P. Gopikrishnan, V. Plerou, L.A. Nunes Amaral, M. Meyer, and H.E. Stanley, Phys. Rev. E **60**, 5305 (1999); A. Chessa, H.E. Stanley, A. Vespignani, and S. Zaperi, *ibid.* **59**, R12 (1999).

[7] P. Bak, *How Nature Works* (Oxford University Press, Oxford, 1997).

[8] *Lévy Flights and Related Topics in Physics*, edited by T.H. Soloman, E.R. Weeks, M.F. Shlesinger, G.M. Zaslavsky, and U. Frisch (Springer, Berlin, 1995).

[9] P. Lévy, *Théorie de l'Addition des Variables Aléatories* (Gauthier-Villars, Paris, 1937).

[10] B.B. Mandelbrot and J.W. van Ness, SIAM Rev. **104**, 422 (1968).

[11] M. Ding and W. Yang, Phys. Rev. E **52**, 207 (1995).

[12] W. Feller. *An Introduction to Probability Theory and Its Applications*, 2nd ed. (Wiley, New York, 1971), Vol. II.

[13] S.T. Bramwell, P.C.W. Holdsworth, and J.-F. Pinton, Nature (London) **396**, 552 (1998).

[14] A. Fournier, D. Fussell, and L. Carpenter, Comm. ACM **25**, 371 (1984).

[15] R.J.A. Tough and K.D. Ward, J. Phys. D **32**, 3075 (1999).

[16] J.H. Jefferson and J.D. Anderson, in *Proceedings of the Conference of the Advisory Group for Aerospace Research and Development* (NATO, Brussels, 1987), Vol. 419, pp. 14.1–14.19.

[17] M. Evans, N. Hastings, and B. Peacock, *Statistical Distributions*, 2nd ed. (Wiley, New York, 1993).

[18] *Handbook of Mathematical Functions*, edited by M. Abramowitz and I.A. Stegun 9th ed., (Dover, New York, 1970).